2.2 VALIDATION OF THE NORTH AMERICAN LAND DATA ASSIMILATION SYSTEM (NLDAS) USING DATA FROM OKLAHOMA MESONET OASIS SITES

Kodi L. Nemunaitis* and Jeffrey B. Basara
Oklahoma Climatological Survey, University of Oklahoma, Norman, OK

Brian A. Cosgrove
SAIC/NASA/Goddard Space Flight Center, Greenbelt, MD

Dag Lohmann
NOAA/NWS/NCEP/EMC, Silver Springs, MD

Ken E. Mitchell
NOAA/NWS/NCEP/EMC, Silver Springs, MD

Paul R. Houser
NASA/Goddard Space Flight Center, Greenbelt, MD

1. INTRODUCTION

Land surface variability is important in many hydrologic and land-atmosphere interactions. Anomalous land surface conditions on a large-scale can lead to droughts or floods, while regional variations can enhance dryline formation and initiate convection. Furthermore, the relative partitioning between latent and sensible heat fluxes at all spatial and temporal scales is controlled largely by variations in land surface conditions. Thus, understanding the spatial and temporal variability in the land surface is vital to determine the influence that land surface processes have upon the atmosphere. Due to its importance in Numerical Weather Prediction (NWP), land surface-atmosphere interactions have been incorporated into forecast models. However, errors in the NWP forcing accumulate in the soil moisture and energy stores, resulting in the incorrect partitioning of latent and sensible heat fluxes.

Currently, a Land Data Assimilation System (LDAS) is being developed at both the North American (NLDAS) and global (GLDAS) scales. It consists of uncoupled models forced with observations, output from NWP models, satellite data, and radar precipitation estimates. NLDAS is currently being developed in partnership between federal and university organizations, seeking to improve the simulation of land surface states and energy fluxes in land-atmosphere numerical models. This project will reduce forecast errors and lead to more accurate reanalysis simulations by NWP and climate models.

The Oklahoma Mesonet is an automated network of 115 remote, meteorological stations across Oklahoma (Brock et al. 1995). It has integrated sensing devices to compliment the standard suite of meteorological and hydrological sensors. In addition to providing observations such as air temperature, relative humidity, station pressure, and wind speed and direction, nearly 100 stations measure the components of the surface energy budget and soil moisture.

This study seeks to validate the NLDAS surface energy budget simulated by the Mosaic and Noah land surface models (LSMs) using the independent observations from the Oklahoma Mesonet. By utilizing the unique land surface observations collected by the Oklahoma Mesonet, improvements can be made to NWP models affecting Oklahoma, North America, and the globe.

2. NLDAS

The NLDAS infrastructure consists of four uncoupled LSMs forced with hourly gauge-based precipitation observations, output from the Eta model data assimilation system (EDAS), solar radiation from the GOES satellites, and radar precipitation estimates. The NLDAS domain covers the continental United States, part of Canada, and part of Mexico or the area between 125°W and 67°W, and between 25°N and 53°N, with a 1/8° latitude-longitude resolution.

The surface forcing data includes 7 primary forcing fields at hourly intervals: air temperature, wind speed, air specific humidity, surface pressure, precipitation, incoming shortwave radiation, and incoming longwave radiation [Cosgrove et al. 2003a]. EDAS, an intermittent assimilation system consisting of successive 3-hr Eta model forecasts and a 3D-variational analysis, is the primary source of the atmospheric forcing fields. However, precipitation and incoming shortwave radiation are provided by actual observations rather than from model output. Precipitation is provided by NCEP's 1/4° daily gauge observations [Shi et al. 2003]. This precipitation field is spatially interpolated to the NLDAS grid and temporally partitioned into hourly fields through the use of WSR-88D Stage II/III precipitation estimates. Incoming shortwave radiation is provided by the 1/2° GOES-based satellite retrieval of incoming shortwave radiation [Pinker et al. 2003]. When these observations are not available, the EDAS precipitation and incoming shortwave radiation serve as backup values. When EDAS is unavailable, forcing data is based on 3-hourly and 6-hourly Eta forecasts.

Corresponding author address:
Kodi L. Nemunaitis, Oklahoma Climatological Survey, 100 E. Boyd St., Suite 1210, Norman, Oklahoma, 73019. E-mail: kodin@ou.edu

The four LSMs implemented in NLDAS are Noah [Pan and Mahrt 1987; Ek et al. 2003], Mosaic [Koster and Suarez 1996], the Variable Infiltration Capacity model (VIC; Liang et al. 1994, 1996a-b; Cherkauer et al. 1999), and the Sacramento Soil Accounting model (SAC; Burnash et al. 1973). Each LSM represents a different approach to land surface modeling. The Noah and Mosaic models are soil-vegetation-atmosphere-transfer (SVAT) schemes used in coupled atmospheric modeling, which simulate land surface temperature, components of the surface energy and water balance equations, snow water equivalent, and soil moisture at various depths. On the other hand, the SAC and VIC models were developed by the hydrologic community as uncoupled hydrology models. Due to their extensive execution in both coupled and uncoupled modes on various spatial scales, the Mosaic, Noah, and VIC LSMs are considered both SVATs and semi-distributed hydrological models. SAC is a storage-type hydrology model which omits the surface energy balance and only simulates the surface water balance. Therefore, it has been omitted from this study. VIC has been widely applied to large continental river basins. Due to the absence of large river basins in Oklahoma the primary models of interest for this preliminary study are the Noah and Mosaic models.

The Mosaic LSM [Koster and Suarez 1996] is an SVAT model developed at NASA GSFC. Mosaic was derived from the Simple Biosphere (SiB) model [Sellars et al. 1986] for coupled use with a global climate model; it accounts for the sub-grid heterogeneity of vegetation and soil moisture through use of a tile or "mosaic" approach. As implemented in LDAS, each grid box may be divided into a maximum of 10 tiles based on a vegetation class that accounts for at least 5% of the grid. The energy and water balance equations, soil moisture, and soil temperature at three soil depths are calculated for each tile. The grid-box mean is evaluated as an areally- weighted mean of each tile within the grid. This Mosaic configuration in NLDAS departs from the standard Mosaic configuration, for the purpose of easier comparison with the soil moisture observation levels of the Oklahoma Mesonet and the soil layers of the VIC and Noah models (e.g. their 10 cm top layer). Although never executed before with fixed layer thickness, Mosaic performed well in the PILPS experiments when configured in the standard way [Chen et al. 1997; Lohmann et al. 1998; Wood et al. 1998]. The standard Mosaic configuration varies the soil type and layer thickness tile by tile according to vegetation type and yields top-down layer thickness ranges of 1-2 cm, 1-150 cm, and 30-200 cm, total column depth ranges of 32-350 cm, and root depths of 2-49 cm for non-forest and 150 cm for forests.

The Noah LSM is an SVAT model initially developed at Oregon State University [Pan and Mahrt 1987]; it was developed for coupled use with NCEP's operational mesoscale Eta model [Chen et al. 1997; Betts et al. 1997; Ek et al. 2003]. Noah was formulated without tiles, yet it effectively reproduces the observed energy and water balances. Furthermore, the Noah model is the only NLDAS LSM to account for both liquid and frozen soil moisture.

3. OBSERVATIONS

A key component of NLDAS development is the validation of model simulations using high-quality, independent observations. A unique tool for this purpose is the Oklahoma Mesonet.

The Oklahoma Mesonet is an automated network of 115 remote, hydrometeorological stations across Oklahoma [Fig. 1; Brock et al. 1995; Shafer et al. 2000]. Each station measures 10 core parameters which include: air temperature and relative humidity at 1.5 m, wind speed and direction at 10 m, barometric pressure, rainfall, incoming solar radiation, bare and vegetated soil temperatures at 5, 10, and 30 cm below ground level, and soil moisture at 5, 25, 60, and 75 cm. The data are collected every 5 minutes as a 5-minute average value, with the exception of soil temperature (15 min) and soil moisture (30 min) data. The Mesonet was installed in 1993 and became operational on 1 January 1994. Since that time, over 3 billion observations have been archived at an archiving frequency that exceeds 99% of the possible observations. Core Mesonet data are collected and transmitted to a central processing facility every 15 minutes where they are quality assured, archived, and distributed [Shafer et al. 2000].

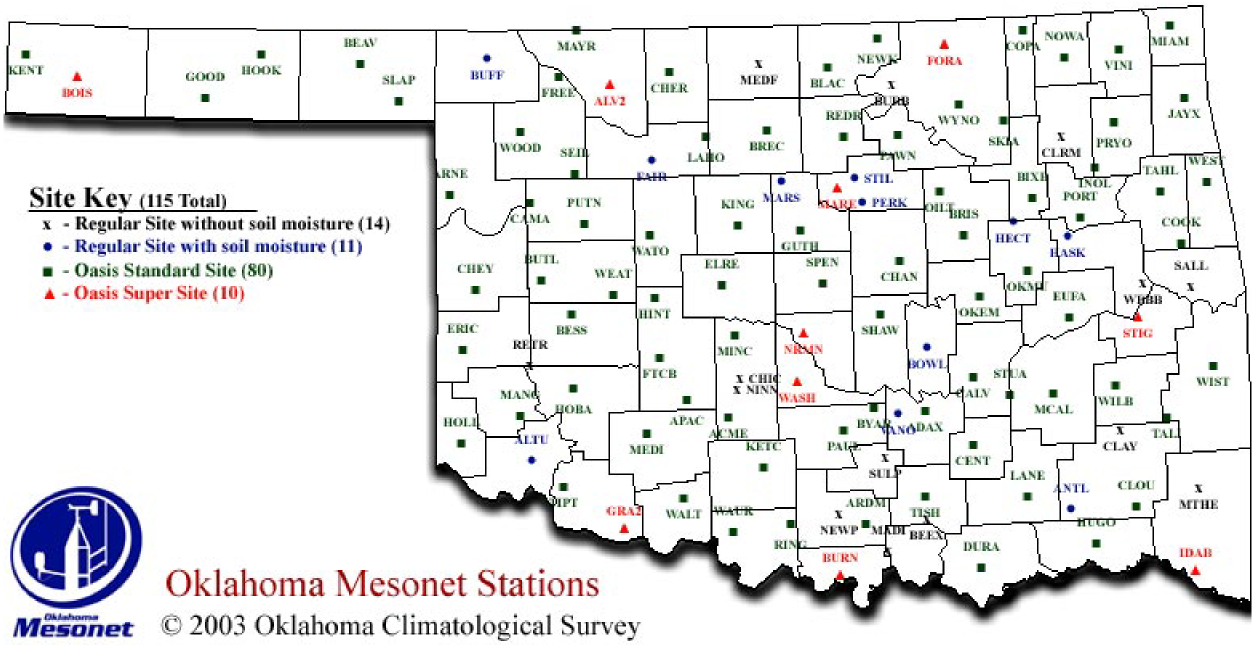

Figure 1: Location of Oklahoma Mesonet Sites in June 2003.

In 1999, the Oklahoma Atmospheric Surface-layer Instrumentation System (OASIS) Project upgraded 89 sites with a suite of instruments capable of estimating the surface energy balance [Brotzge et al. 1999; Basara and Crawford 2002]. In addition, OASIS Super Sites, a subset of 10 OASIS sites, were instrumented to measure the components of the surface energy balance with enhanced accuracy. The 10 OASIS Super Sites measure latent and sensible heat fluxes using eddy covariance techniques, ground heat flux, the four components of net radiation, and skin temperature. Each Super Site is located in a different climate region of Oklahoma and, as a permanent installation, permits the investigation of a wide range of atmospheric conditions over extended periods of time.

Net radiation at the 89 standard OASIS sites is measured at 1.5 m using the Kipp & Zonen NR-Lite [Brotzge et al. 1999]. The NR-Lite measures the sum of incoming and outgoing shortwave and longwave radiation. Sensible heat flux is estimated using a profile technique [Brotzge and Crawford 2000] whereby sensors measure the vertical gradients of temperature and wind speed. Then, Monin-Obukov similarity theory is applied to the temperature and wind gradients to estimate sensible heat flux. Ground heat flux is estimated using a combination method [Tanner 1960] that uses measurements of soil heat flux and soil heat storage. Because net radiation, sensible heat flux, and ground heat flux are measured at each site, latent heat flux is estimated as the residual term in the surface energy balance equation:

$$R_{net} = LE + H + G \qquad (1)$$

Surface skin temperature is measured at 2 m using an infrared thermocouple temperature sensor manufactured by Apogee [Fiebrich et al. 2003].

Sensors at the OASIS Super Sites estimate the surface energy balance using the same instruments and techniques as those at the standard OASIS sites. In addition, the Super Sites measure net radiation at 1.5 m using a 4-component CNR1 radiometer. As such, incoming and outgoing shortwave and longwave radiation are measured explicitly. Furthermore, the sensible and latent heat fluxes are measured directly via an eddy correlation approach using a CSI CSAT3 sonic anemometer and Krypton hygrometer are installed at 4.5 m above ground.

The primary observations included net radiation, downwelling shortwave radiation, reflected shortwave radiation, downwelling longwave radiation, upwelling longwave radiation, sensible heat flux, latent heat flux, ground heat flux, and skin temperature. Initially, time-series plots of downwelling shortwave radiation data were analyzed to identify "candidate days". Candidate days are days when the land-atmosphere interaction is the dominant forcing mechanism of the near-surface atmosphere (i.e., little or no cloud cover present, with weak wind shear in the lower troposphere). Once candidate days in 2000 were determined, time series plots of net radiation, latent heat flux, sensible heat flux, and ground heat flux were created. An example of a time series plot from a typical "sunny-day" profile illustrates downwelling shortwave radiation and the land-surface flux components of the surface energy budget (Fig. 2). Upon examination of all dates in 2000, a total of 475 case-study days were identified across the network. Initial quality-assurance (QA) methods were developed to determine errors associated with the OASIS flux data. First, candidate days during 2000 were examined with priority placed upon dates when all ten sites met the candidate day criteria. The data were quality assured by visually inspecting the radiation and heat flux time-series plots for each site while scanning the data one observation at a time to assign quality assurance flags to the data.

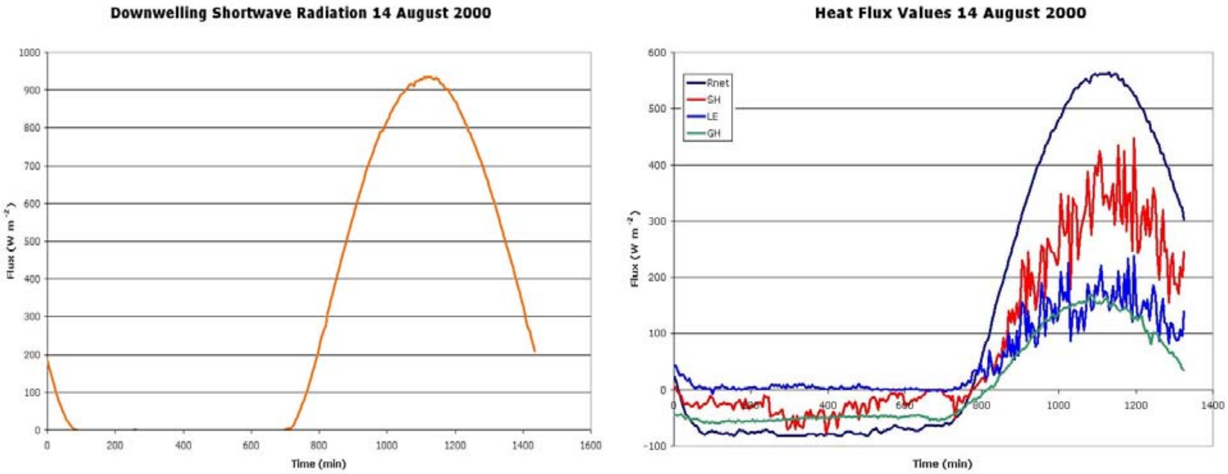

Figure 2. Time Series Plots of Downwelling Shortwave Radiation and Components of the Surface Energy Budget at the NORM Mesonet Site for August 14, 2000.

The quality assurance flags for each datum were: 0 = good, 1 = suspect, 2 = warning, 3 = bad or missing data. Because latent heat flux depended upon output from the sonic anemometer which was used (in part) to measure sensible heat flux values, it was necessary to flag latent heat flux values when sensible heat flux measurements were flagged.

The QA of skin temperature data included ensuring the sensor body temperature of the infrared temperature sensor (IRT) was within the calibrated range. Thus, skin temperature values less than 5°C or greater than 45°C were flagged with a value of 3 and removed from the analysis.

Using this methodology, data from 17 days were quality assured to include data from all ten OASIS Super Sites during 2000. Due to the tedious nature of these quality assurance procedures, automated methods are being developed to quality assure data from the Super Sites. Because this data was collected and archived beginning on 1 June 1999 for ten sites, thousands of research-quality candidate days possibly exist for analysis.

4. ANALYSIS

Using retrospective simulation data provided by the NLDAS Group from the Mosaic and Noah LSMs, surface energy fluxes were simulated for the summer of 2000. The model simulated energy fluxes were compared with OASIS surface data, such as net radiation, upwelling and downwelling shortwave radiation, upwelling and downwelling longwave radiation, latent heat flux, sensible heat flux, ground heat flux, and skin temperature. The 5-minute values of OASIS Super Site data were averaged into hourly mean values provided that 75% or more of the data for each hour were not flagged as bad or missing.

4.1 Net Radiation

Net radiation at all OASIS Super Sites were compared with corresponding values at nearby grid points from the Mosaic and Noah LSMs (Fig. 4a-d). The comparison of net radiation between Mosaic model output and OASIS data demonstrate that the simulated values of the diurnal cycle were very consistent with the observed values. However, the Mosaic model tended to produce larger diurnal amplitudes than those observed; the largest differences occurred in net radiation during the late summer. Even so, the discrepancies between the observed and modeled values were minor with the difference in magnitude generally less than 60 W m^{-2}. The results of the comparison of net radiation between modeled by Noah and observed by OASIS revealed consistent agreement throughout the data set for each Super Site. However, the mean net radiation curve for the Noah LSM had a thirty-minute phase difference in the diurnal cycle. As a result, Noah peaked earlier than did the values from observations. In addition, the magnitude of the peak values of the modeled net radiation was less than the peak observed values. Finally, this study demonstrated that the phase lag of the diurnal cycle of net radiation between Noah and the OASIS observations was most pronounced during early summer and diminished as the season progressed.

a. b.

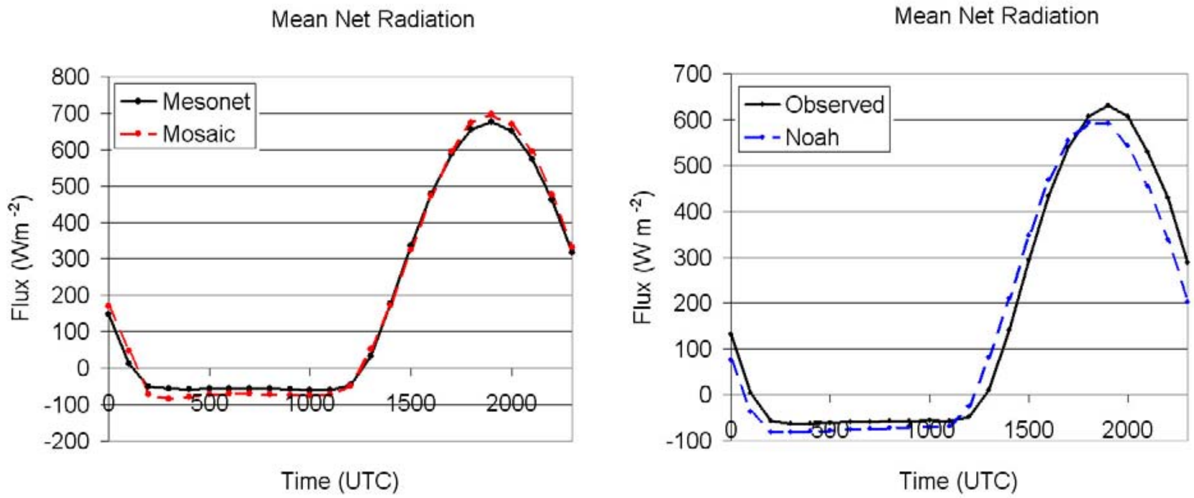

Figure 3. The mean diurnal cycle of net radiation for candidate days during the summer of 2000 at both OASIS Super Sites and corresponding (a) Mosaic and (b) Noah grid points.

4.2 Components of Net Radiation

Net radiation is comprised of upwelling and downwelling longwave and shortwave radiation. As a result, it is critical to investigate the components of the radiation budget because errors in each component impacted the energy available to the surface energy balance. The comparison of downwelling shortwave radiation at OASIS Super Sites with corresponding model values is shown in Figure 4. While the Mosaic modeled and observed curves represent the same diurnal pattern, a slight underestimate of downwelling shortwave radiation during the initial daytime hours and an overestimate during the late daytime hours was observed when compared to the observations. In addition, differences of approximately 20 W m^{-2} were consistently observed across Oklahoma. Finally, as was the case with total net radiation, the modeled values of downwelling shortwave radiation computed by the Noah LSM exhibited a thirty-minute phase difference when compared with the OASIS observations. Robock et al. (2003) attributed the phase error in downwelling solar radiation to the use of a non-optimal technique for projecting the observed solar forcing at hourly intervals onto the model's physical time step.

a. b.

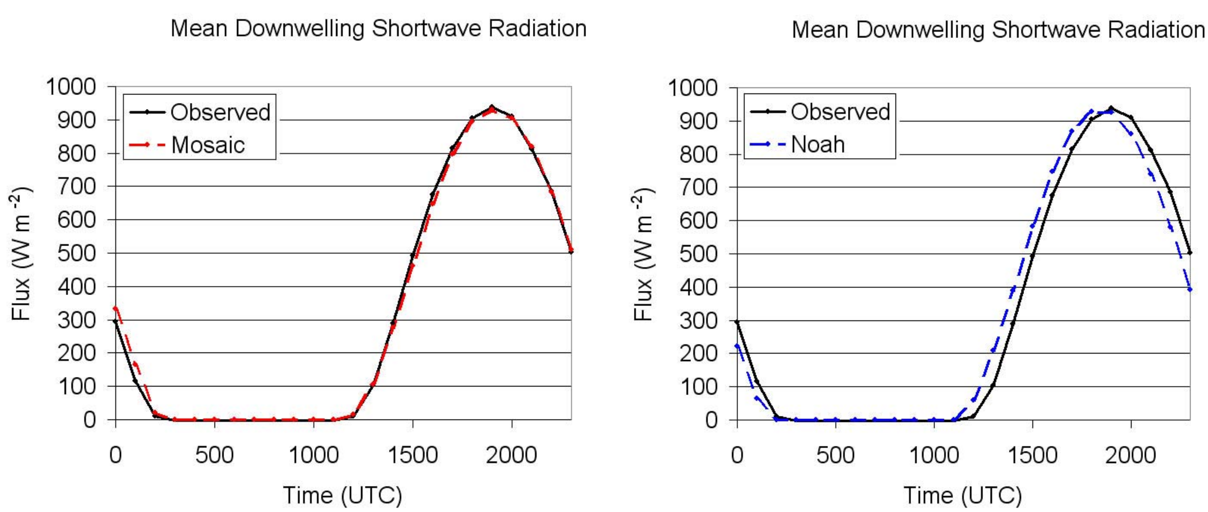

Figure 4. The mean diurnal cycle of downwelling shortwave radiation for candidate days during the summer of 2000 at both OASIS Super Sites and corresponding (a) Mosaic and (b) Noah grid points.

a. b.

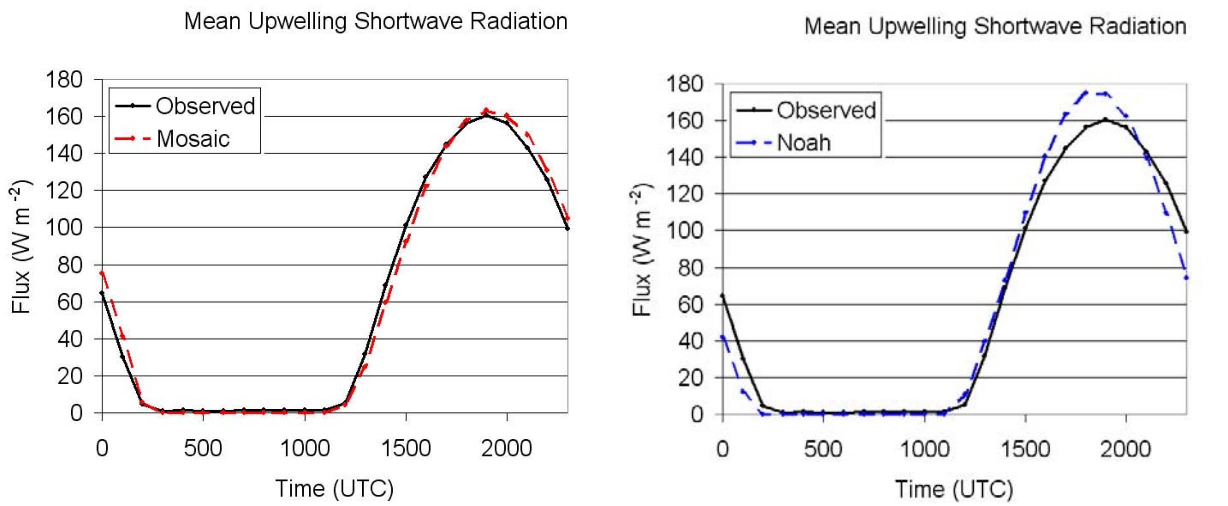

Figure 5. The mean diurnal cycle of upwelling shortwave radiation for candidate days during the summer of 2000 at both OASIS Super Sites and corresponding (a) Mosaic and (b) Noah grid points.

Relative to net radiation and downwelling shortwave radiation, the comparison between observed and modeled upwelling shortwave radiation revealed slightly larger discrepancies (Fig. 5). The Mosaic LSM results produced slight inconsistencies between the modeled and observed mean diurnal cycle. In addition, the Mosaic model tended to underestimate the upwelling shortwave radiation during the daytime hours early in the summer and to overestimate upwelling shortwave radiation late in the summer. The time series of upwelling shortwave radiation produced by the Noah model and the time series of the observations were significantly different (Fig. 5b). The modeled curve overestimated peak daytime values and did so too early in the day; thereafter, the model decreased its forecast radiation at a faster rate than the observations. These results were consistent throughout the study period at all sites and did not appear to have any temporal pattern with respect to seasonal changes.

The downwelling longwave radiation at the OASIS Super Sites was compared with the corresponding values at grid points from the Mosaic and Noah LSMs (Fig. 6). The results revealed an underestimation of downwelling radiation by both the Mosaic and Noah models compared to the observations. The underestimation of downwelling longwave radiation noted in this study was consistent with biases in NLDAS forcing presented by Luo et al. (2003). They surmised that this may result from an underestimate of downward longwave radiation from EDAS, a result that also is consistent with other validation studies [Betts et al. 1997; Hinkelman et al. 1999; Berbery et al. 1999].

a. b.

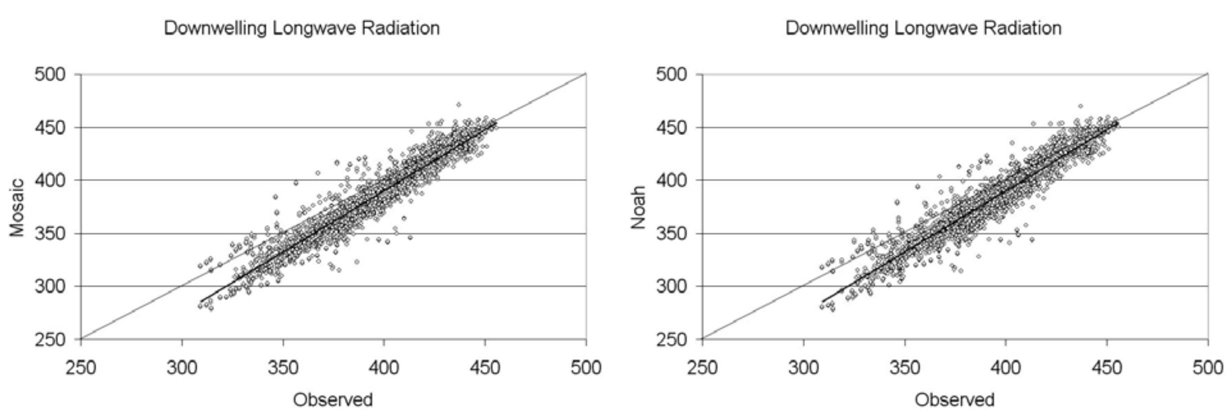

Figure 6. The scatter plot of downwelling longwave radiation at OASIS Super Sites and corresponding (a) Mosaic and (b) Noah model grid points.

a. b.

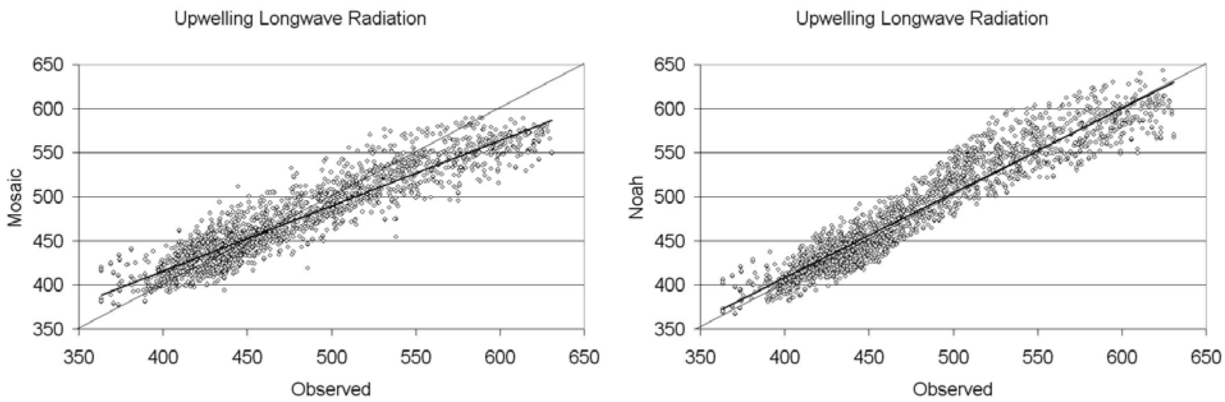

Figure 7. The scatter plot of upwelling longwave radiation at OASIS Super Sites and corresponding (a) Mosaic and (b) Noah model grid points.

a. b.

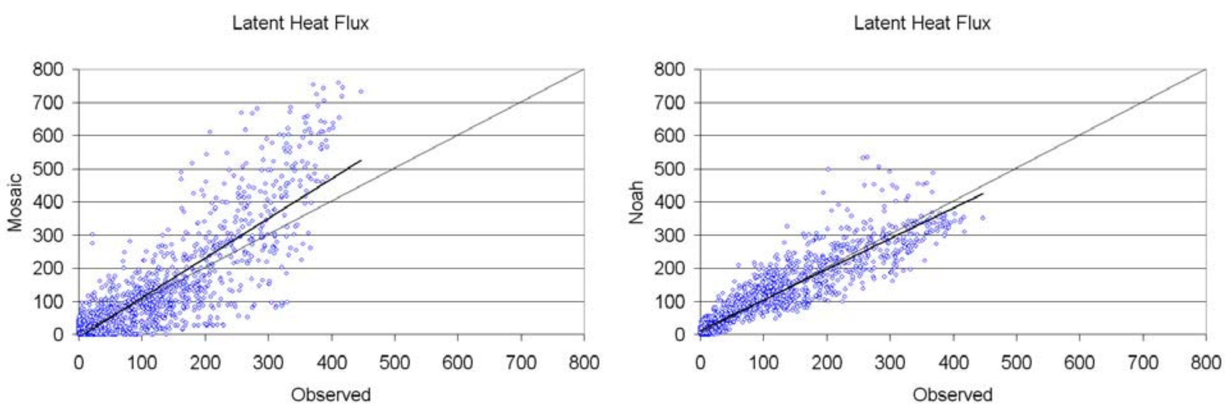

Figure 8. The scatter plot of latent heat flux at OASIS Super Sites and corresponding (a) Mosaic and (b) Noah model grid points.

The comparison of upwelling longwave radiation at OASIS Super Sites with corresponding model values is shown in Figure 7. The Mosaic model overestimated upwelling longwave radiation during the nighttime hours and underestimated upwelling longwave radiation during the daytime. In the case of the Noah LSM, upwelling longwave radiation was slightly overestimated.

4.3 Surface Fluxes

Because LSMs use parameterizations and related techniques to represent the physical exchange of mass and energy between the land surface and the atmosphere, LSMs partition the available radiative energy into latent, sensible, and ground heat fluxes in different manners. As such, it is critical to validate the model derived fluxes with trustworthy observations over varying soil, vegetation, and climate regimes.

The results of an intercomparison between observed surface fluxes and those produced by the Mosaic LSM reveal discrepancies larger than those uncovered for net radiation and the components of net radiation. For example, the Mosaic LSM consistently overestimated latent heat flux in the late afternoon when compared with OASIS observations (Fig. 8). The observed fluxes typically increased more rapidly and peaked earlier than did the modeled fluxes. Furthermore, the modeled latent heat flux values were approximately 30 W m^{-2} larger than the observed values. Conversely, it was common for the latent heat flux simulated by the Noah model to display a 30-minute phase difference when compared with the observed values. When the phase difference was taken into account, the results also revealed a slight underestimation of the latent heat flux values by the Noah LSM compared to observations collected across Oklahoma.

The flux of sensible heat at the OASIS Super Sites was compared with corresponding model values (Fig. 9). The values of sensible heat flux produced by the Mosaic LSM correlated very poorly with the observed values as illustrated in Figure 9a. Furthermore, the Mosaic LSM significantly underestimated daytime fluxes of sensible heat while the nighttime flux of sensible heat was overestimated. In addition, the underestimate of sensible heat flux during daytime hours improved from the spring through the summer. However, the overestimate of sensible heat flux during the nighttime hours worsened from spring through the summer months. The results in Figure 9 also revealed increased correlation between sensible heat flux produced by the Noah model and the OASIS observations compared to similar analyses between observations and fluxes from the Mosaic LSM. Even so, the intercomparisons revealed that sensible heat fluxes from the Noah model were greater than observed values. However, the magnitude of difference was a function of time of year. For example, the discrepancies improved from May to August 2000 as the overall magnitude of sensible heat flux increased. Finally, the phase between observations and concurrent Noah values also occurred in the diurnal cycle of sensible heat flux.

The largest discrepancies between OASIS observations and modeled values of components of the surface energy budget were between the Mosaic LSM and observations of ground heat flux. The ground heat flux from Mosaic contained a strong bias as the Mosaic LSM consistently overestimated flux values at all hours of the day (Fig. 11). In some cases, the differences between OASIS observations and Mosaic values exceeded 300 W m^{-2}! The strong bias between OASIS and Mosaic fluxes also has been documented by Robock et al. (2003) who determined that, while Mosaic modeled ground heat flux were overestimated during the summer, they were underestimated during the winter. Conversely, the ground heat flux values computed by Noah compared well with OASIS observations. Even so, the diurnal cycle of the values of Noah modeled ground heat flux generally had a larger diurnal amplitude than the observations and a phase difference in the diurnal cycle was also observed.

As noted by Mitchell et al. (2003), the strong biases seen in the Mosaic ground heat flux fields can be attributed to the value of the soil heat capacity parameter (C_H) used in the Mosaic LSM. In NLDAS, the C_H value in Mosaic's Retrospective run (175,000 J m^{-2} K^{-1}) was one calibrated in an earlier, independent temperature data assimilation system [Radakovich et al. 2001], and not the lower traditional C_H value (70,000 J m^{-2} K^{-1}) specified by Koster and Suarez (1996) and used in several Mosaic PILPS experiments. To gauge the

a. b.

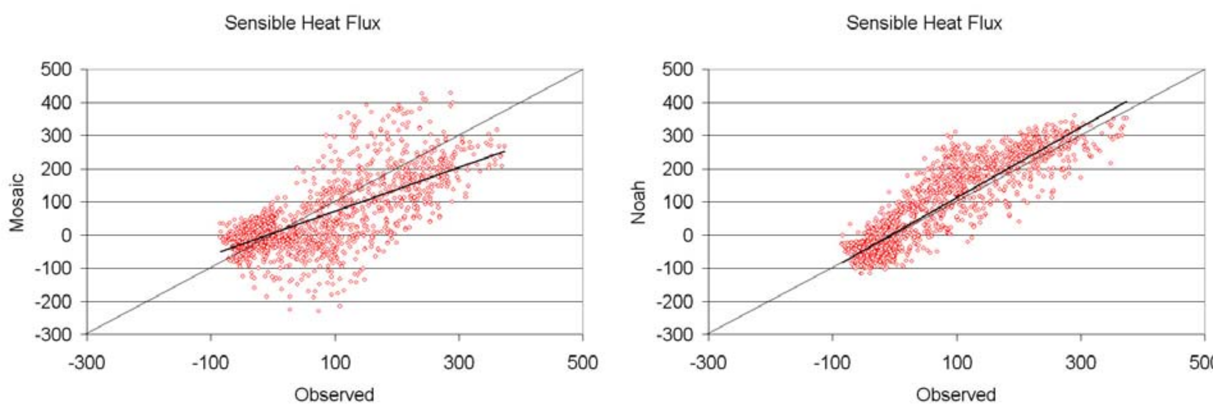

Figure 9. The scatter plot of sensible heat flux at OASIS Super Sites and corresponding (a) Mosaic and (b) Noah model grid points.

a. b.

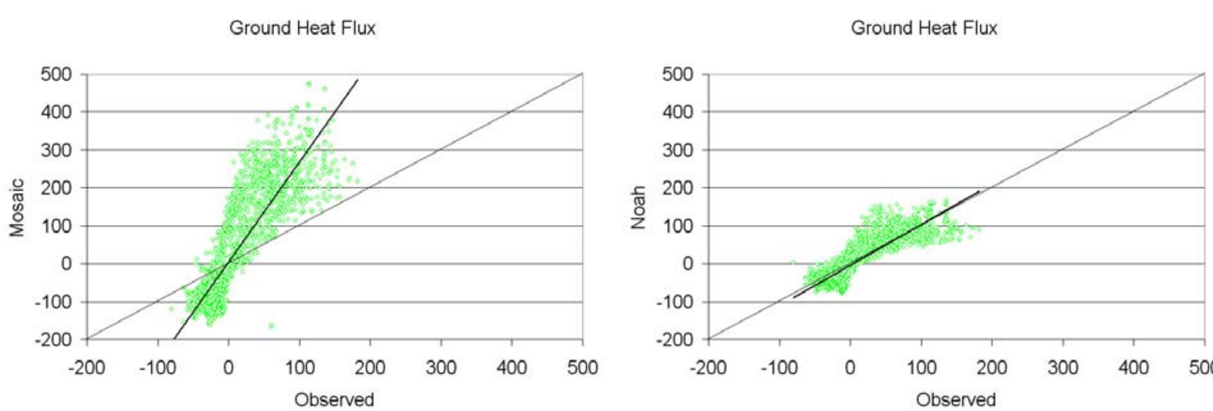

Figure 10. The scatter plot of ground heat flux at OASIS Super Sites and corresponding (a) Mosaic and (b) Noah model grid points.

impact of C_H, a Mosaic test was executed in NLDAS using the traditional lower value. Ground heat flux values were dramatically improved in the test, becoming competitive with that in Noah (though Mosaic manifests an unusual anomaly in ground heat flux during the early morning). This improvement in simulated ground heat flux holds throughout the year.

4.4 Skin Temperature

The Mosaic, Noah, and VIC NLDAS LSMs calculate an average surface temperature, referred to as skin temperature. The OASIS Super Site IRT observations were compared to the average values of the model-estimated surface temperatures (Fig. 11). The Mosaic LSM had a daytime cool bias and nighttime warm bias. These results were consistent with the overestimate of upwelling longwave radiation during nighttime hours and the underestimate during the daytime because skin temperature is derived from upwelling longwave radiation via the Stephan-Boltzmann Law. Even so, the Mosaic LSM repeatedly underestimated the overall magnitude of upwelling longwave radiation. Also, the large underestimate in skin temperature by the Mosaic LSM can be expected given the high biases in latent and ground heat fluxes (which efficiently cool the surface) and the low bias in sensible heat flux (reduced warming of surface temperatures). The comparison between the Noah model and the observations revealed a warm bias in skin temperature during daylight hours. These results were also consistent with the slight daytime high bias in upwelling longwave radiation (yielding increased surface temperatures) and can be seen by comparing Figures 7 and 11. Mitchell et al. (2003) attributed part of this daytime bias to a value of aerodynamic conductance that is too small.

5. CONCLUSIONS

The validation of the radiation and surface energy budgets simulated by the Mosaic and Noah LSMs using OASIS data provides a blueprint for future work. In terms of a regional approach, these results demonstrated that the physical nature of net radiation is captured very well by both models. However, forcing biases were evident in the intercomparisons of downwelling shortwave and longwave radiation. In addition, a phase error in the Noah downwelling shortwave radiation due to the use of a non-optimal technique for projecting the input hourly solar forcing onto the model physical time step was evident in the analyses. The upwelling shortwave and longwave radiation intercomparisons revealed differences between the model output and the observations. Upwelling longwave radiation was underestimated by the Mosaic model and overestimated by the Noah model during daylight hours.

The intercomparisons of latent heat flux revealed significant differences between the model output and the observations. Mosaic produced greater flux values than the observations while Noah produced smaller flux values than those measured. Sensible heat fluxes compared less favorably. Sensible heat flux values were overestimated by the Noah model and greatly underestimated by the Mosaic model. Additionally, the Mosaic land surface model consistently overestimated ground heat flux compared to the observed values, in part due to the value of C_H used in the model. However, ground heat flux values were only slightly overestimated by the Noah model. Finally, the skin temperature results were consistent with those of upwelling longwave radiation. The Mosaic LSM produced a daytime cool bias while the Noah LSM produced a slight daytime warm bias.

Future analyses will build upon the results demonstrated in this study. Further investigations of additional candidate days and closer inspection of individual sites will allow for a more complete validation effort. In turn, Noah and Mosaic model performance will be improved.

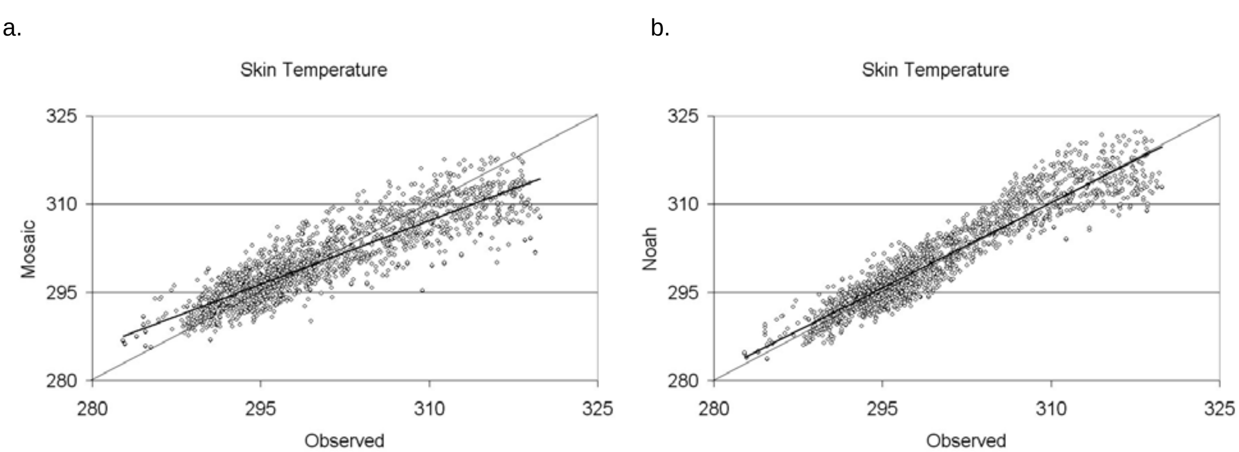

Figure 11. The scatter plot of skin temperature at OASIS Super Sites and corresponding (a) Mosaic and (b) Noah model grid points.

ACKNOWLEDGEMENTS
This research was made possible, in part, by a NASA-EPSCOR Research Initiation Grant, an NSF MRI grant (ATM-9724594) which provided funds to add sensors to measure the radiation and energy budgets at Oklahoma Mesonet sites, and support from the NOAA Office of Global Programs (NOAA grant number NA17RJ1227).

REFERENCES

Basara, J. B., and K. C. Crawford, 2002: Linear relationships between root-zone soil moisture and atmospheric processes in the planetary boundary layer. *J. Geophys. Res.*, **107**, 10, 1-18.

Basara, J. B., 2001: The value of point-scale measurements of soil moisture in planetary boundary layer simulations. Ph.D. dissertation, School of Meteorology, University of Oklahoma, 15-30.

Berbery, E., K. Mitchell, S. Benjamin, T. Smirnova, H. Ritchie, R. Hogue, and E. Radeva, 1999: Assessment of land-surface energy budgets from regional and global models. *J. Geophys. Res*., **104**, 19329-19348.

Betts, A., F. Chen, K. Mitchell, and Z. Janjic, 1997: Assessment of the land surface and boundary layer models in two operational versions of the NCEP Eta model using FIFE data. *Mon. Wea. Rev.*, **125**, 2896-2916.

Brock, F. V., K. C. Crawford, R. L. Elliott, G. W. Cuperus, S. J. Stadler, H. L. Johnson, and M. D. Eilts, 1995: The Oklahoma Mesonet: A technical overview. *J. Atmos. Oceanic Technol.*, **12**, 5-19.

Brotzge, J. A., 2000: Closure of the surface energy budget. Ph.D. dissertation, School of Meteorology, University of Oklahoma, Norman.

Brotzge, J. A. and K. C. Crawford, 2000: Estimating Sensible Heat Flux from the Oklahoma Mesonet. *J. Appl. Meteor.*, **39**, 102-116.

Brotzge, J. A., S. J. Richardson, K. C. Crawford, T. W. Horst, F. V. Brock, K. S. Humes, Z. Sorbjan, and R. L. Elliott, 1999: The Oklahoma Atmospheric Surface-layer Instrumentation System (OASIS) Project. Preprints, *13th Conf. on Bound.-Lay. Turb.*, Dallas, TX, Amer. Meteor. Soc., 612-615.

Burnash, R. J. C., R. L. Ferral, and R. A. McGuire, 1973: A generalized streamflow simulation system: conceptual models for digital computers, Joint Fed.-State River Forecast Center, Sacramento, CA.

Chen, T. H., A. Henderson-Sellers, P. C. D. Milly, A. J. Pitman, A. C. M. Beljaars, and 38 others, 1997: Cabauw experimental results from the Project for Intercomparison of Landsurface Parameterization Schemes (PILPS). *J. Climate*, **10**, 1194-1215.

Chen, F., K. E. Mitchell, J. C. Schaake, Y. Xue, H.-L. Pan, V. Koren, Q. Y. Duan, M. Ek, and A. Betts, 1996: Modeling of land-surface evaporation by four schemes and comparison with FIFE observations. *J. Geophys. Res.*, **101**, 7251-7268.

Cherkauer, K. A., and D. P. Lettenmaier, 1999: Hydrologic effects of frozen soils in the upper Mississippi River basin, *J. Geophys. Res.*, **104**, 19, 599-19,610.

Cosgrove, B. A., D. Lohmann, C. H. Marshall, K. E. Mitchell, P. R. Houser, E. F. Wood, J. C. Schaake, A. Robock, J. Sheffield, Q. Duan, L. Luo, R. W. Higgins, R. T. Pinker, J. D. Tarpley, J. Meng, 2003a: Realtime and retrospective forcing in the North American Land Data Assimilation System (NLDAS) project. *J. Geophys. Res.*, in press.

Cosgrove, B. A., K. E. Mitchell, P. R. Houser, E. F. Wood, J. C. Schaake, A. Robock, D. Lohmann, J. Sheffield, Q. Duan, L. Luo, R. W. Higgins, R. T. Pinker, J. D. Tarpley, 2003b: Land surface model spin-up behavior in the North American Land Data Assimilation System (NLDAS). *J. Geophys. Res.*, in press.

Ek, M. B., K. E. Mitchell, Y. Lin, P. Grunmann, E. Rogers, G. Gayno, V. Koren, 2003: Implementation of the upgraded Noah land-surface model in the NCEP operational mesoscale Eta model. *J. Geophys. Res.*, (submitted).

Fiebrich, C. A., J. E. Martinez, J. A. Brotzge, and J. B. Basara, 2003: The Oklahoma Mesonet's skin temperature network. *J. Atmos. Oceanic Tech*., in press.

Hinkelman, L. M., T. P. Ackerman, and R. T. Marchaud, 1999: An evaluation of NCEP Eta model predictions of surface energy and cloud properties by comparison with measured ARM data. *J. Geophys. Res.*, **104**, 19535-19550.

Koster, R., and M. Suarez, 1996: Energy and Water Balance Calculations in the Mosaic LSM. *NASA Tech Memo*, 104606, **9**.

Liang, X., D. P. Lettenmaier, and E. F. Wood, 1996a: One-dimensional statistical dynamic representation of subgrid spatial variability of precipitation in the two-layer variable infiltration capacity model, *J. Geophys. Res.*, **101**, 21, 403-21,422.

Liang, X., E. F. Wood, and D. P. Lettenmaier, 1996b: Surface soil moisture parameterization of the VIC-2L model: Evaluation and modifications, *Glob. Planet. Change*, **13**, 195-206.

Liang, X., D. P. Lettenmaier, E. F. Wood, and S. J. Burges, 1994: A simple hydrologically based model of land surface water and energy fluxes for GCMs. *J. Geophys Res.*, **99**, 14, 415-14, 428.

Lohmann, D., K. E. Mitchell, P. R. Houser, E. F. Wood, J. C. Schaake, A. Robock, B. A. Cosgrove, J. Sheffield, Q. Duan, L. Luo, R. W. Higgins, R. T. Pinker, J. D. Tarpley, 2003: Streamflow and water balance intercomparison of four land-surface models in the North American Land Data Assimilation System (NLDAS), *J. Geophys. Res.*, (submitted).

Lohmann, D., D. P. Lettenmaier, X. Liang, E. F. Wood, A. Boone, S. Chang, F. Chen, Y. Dai, C. Desborough, R. E. Dickinson, Q. Duan, M. Ek, Y. M. Gusev, F. Habets, P. Irannejad, R. Koster, K. E. Mitchell, O. N. Nasonova, J. Noilhan, J. Schaake, A. Schlosser, Y. Shao, A. B. Shmakin, D. Verseghy, K. Warrach, P. Wetzel, Y. Xue, Z.-L. Yang, Q.-C. Zeng, 1998: The project for intercomparison of land-surface parameterization schemes (PILPS) phase 2(c) Red--Arkansas River basin experiment: 3. Spatial and temporal analysis of water fluxes, *Glob. Planet. Change*, **19**, 161-179.

Mitchell, K. E., D. Lohmann, P. R. Houser, E. F. Wood, J. C. Schaake, A. Robock, B. A. Cosgrove, J. Sheffield, Q. Duan, L. Luo, R. W. Higgins, R. T. Pinker, J. D. Tarpley, D. P. Lettenmaier, C. H. Marshall, J. K. Entin, M. Pan, W. Shi, V. Koren, J. Meng, B. H. Ramsay, and A. A. Bailey, 2003: The Multi-institution North American Land Data Assimilation System (NLDAS) Project: Utilizing multiple GCIP products and partners in a continental distributed hydrological modeling system. *J. Geophys. Res.* (submitted).

Pan, H.-L., and L. Mahrt, 1987: Interaction between soil hydrology and boundary layer development. *Boundary-Layer Meteorol.*, **38**, 185-202.

Pinker, R. T., J. D. Tarpley, I. Laszlo, K. E. Mitchell, P. R. Houser, E. F. Wood, J. C. Schaake, A. Robock, D. Lohmann, B. A. Cosgrove, J. Sheffield, Q. Duan, L. Luo, R. W. Higgins, 2003: Surface radiation budgets in support of the GEWEX Continental Scale International Project (GCIP) and the GEWEX Americas Prediction Project (GAPP), including the North American Land Data Assimilation System (NLDAS) Project. *J. Geophys. Res.*, in press.

Radakovich, J. D., P. R. Houser, A. da Silva, and M. G. Bosilovich, 2001: Results from global land-surface data assimilation methods, AMS 5th Symposium on Integrated Observing Systems, Albuquerque, NM, 14-19 January, 132-134.

Robock, A., L. Luo, E. F. Wood, F. Wen, K. E. Mitchell, P. R. Houser, J. C. Schaake, D. Lohmann, B. A. Cosgrove, J. Sheffield, Q. Duan, R. W. Higgins, R. T. Pinker, J. D. Tarpley, J. B. Basara, and K. C. Crawford, 2003: Evaluation of the North American Land Data Assimilation System over the Southern Great Plains during the warm season. *J. Geophys. Res.*, in press.

Sellers, P., Y. Mintz, Y. Sud, and A. Dalcher, 1986: A simple biosphere model (SiB) for use within general circulation models. *J. Atmos. Sci.*, **43**, 505-531.

Shafer, M. A., C. A. Fiebrich, D. S. Arndt, S. E. Fredrickson, and T. W. Hughes, 2000: Quality assurance procedures in the Oklahoma Mesonet. *J. Atmos. Oceanic Tech*., **17**, 474-494.

Shi, W., R. W. Higgins, E. Yarosh, 2003: A unified Raingauge dataset and multi-year daily precipitation reanalysis for the United States. *J. Geophys. Res.*, (submitted).

Tanner, C. B., 1960: Energy balance approach to evapotranspiration from crops. *S. Sci. Soc. of Amer. Proc*., **24**, 1-9.

Wood, E., D. Lettenmaier, X . Liang, D. Lohmann, A. Boone, S. Chang, F. Chen, Y. Dai, R. Dickinson, Q. Duan, M. Ek, Y. Gusev, F. Habets, P. Irannejad, R. Koster, K. Mitchell, O. Nasonova, J. Noilhan, J. Schaake, A. Schlosser, Y. Shao, A. Shmakin, D. Verseghy, K. Warrach, P. Wetzel, Y. Xue, Z. Yang, and Q. Zeng, 1998: The Project for Intercomparison of Land-surface Parameterization Schemes (PILPS) Phase 2(c) Red-Arkansas River basin experiment: 1. Experimental description and summary intercomparisons, *Glob. Planet. Change*, **19**, 115-136.